

Buffered climate change effects in a Mediterranean pine species: range limit implications from a tree-ring study

Juan Carlos Linares · Pedro Antonio Tíscar

Received: 21 October 2010 / Accepted: 25 April 2011 / Published online: 12 May 2011
© Springer-Verlag 2011

Abstract Within-range effects of climatic change on tree growth at the sub-regional scale remain poorly understood. The aim of this research was to use climate and radial-growth data to explain how long-term climatic trends affect tree growth patterns along the southern limit of the range of *Pinus nigra* ssp. *salzmannii* (Eastern Baetic Range, southern Spain). We used regional temperature and precipitation data and measured sub-regional radial growth variation in *P. nigra* forests over the past two centuries. A dynamic factor analysis was applied to test the hypothesis that trees subjected to different climates have experienced contrasting long-term growth variability. We defined four representative stand types based on average temperature and precipitation to evaluate climate–growth relationships using linear mixed-effect models and multi-model selection criteria. All four stand types experienced warming and declining precipitation throughout the twentieth century. From the onset of the twentieth century, synchronised basal-area increment decline was accounted for by dynamic factor analysis and was related to drought by climate–growth models; declining basal-area increment

trends proved stronger at lower elevations, whereas temperature was positively related to growth in areas with high rainfall inputs. Given the contrasting sub-regional tree-growth responses to climate change, the role of drought becomes even more complex in shaping communities and affecting selection pressure in the Mediterranean mountain forests. Potential vegetation shifts will likely occur over the dry edge of species distributions, with major impacts on ecosystem structure and function.

Keywords Basal-area increment · Drought · Dynamic factor analysis · Growth decline · *Pinus nigra* ssp. *salzmannii*

Introduction

Temperature increases and variations in rainfall patterns are main components of climate change (IPCC 2007). Such changes have the potential to profoundly alter the dynamics of drought-sensitive tree species in the Mediterranean mountain forests (Macias et al. 2006; Sarris et al. 2007, 2010; Peñuelas et al. 2007; Andreu et al. 2007). The southernmost European mountain forests in Andalusia (southern Spain) are perhaps among the most vulnerable areas for the loss of tree species due to climate change. Indeed, several recent studies focusing on tree growth and distribution in the Iberian Mediterranean mountains have reported declining tree-growth trends related to temperature rise and drought (Jump et al. 2006; Macias et al. 2006; Andreu et al. 2007; Martínez-Vilalta et al. 2008). Past climate-warming events seem to have promoted shifts in plant species and biomes towards the poles or higher altitudes (Taberlet and Cheddadi 2002). However, the extent of current forest vulnerability to climate change presents

Communicated by Russell Monson.

Electronic supplementary material The online version of this article (doi:10.1007/s00442-011-2012-2) contains supplementary material, which is available to authorized users.

J. C. Linares (✉)
Departamento de Sistemas Físicos, Químicos y Naturales,
Universidad Pablo de Olavide, Ctra. Utrera km. 1,
41002 Sevilla, Spain
e-mail: jclincal@upo.es

P. A. Tíscar
Centro de Capacitación y Experimentación Forestal,
23470 Cazorla, Spain

large uncertainties, and within-range tree responses to regional warming and extreme drought events remain poorly understood.

Relict tree species can serve as models to assess the effects of temperature increase and changing regional rainfall patterns, since such trees may be more growth sensitive to climatic stress (Linares et al. 2010, 2011). To explore the interaction of temperature and precipitation changes and their impact on forest ecosystems, we focus on the southern distribution area of *Pinus nigra* ssp. *salzmannii* (Pyrenean Pine), a drought-sensitive Mediterranean mountain pine (Linares and Tíscar 2010). We assume that tree vulnerability to a given type of climate change is determined mainly by inherent drought sensitivity and adaptive capacity to local conditions and that the correlation between radial growth of dominant trees and climatic variables can be used as a surrogate for species vulnerability to climate change (Ogle et al. 2000; Das et al. 2007; van Mantgem et al. 2009). To study the interaction between temperature and precipitation changes, we selected populations growing under cooler- and warmer-than-average temperatures as well as wetter- and drier-than-average precipitation, and with this information we generated a full factorial design that accounts for long-term climate–growth relationships in the nineteenth and twentieth centuries.

As the starting point, our hypothesis was that regional temperature increase might exacerbate the vulnerability of trees to extreme drought events. To test this, we calculated long-term regional climatic trends related to water deficit (temperature, precipitation, and a drought index) and long-term climate–growth responses. Our specific aims were as follows: (1) to quantify relationships of basal-area increment and climate for *P. nigra* during the nineteenth and twentieth centuries, and (2) to analyse the sub-regional variability in climate–growth relationships and the sensitivity to climatic variability along the southernmost distribution area of *P. nigra*.

Materials and methods

This study was carried out in the Sierra de Cazorla, Segura y Las Villas Natural Park (Fig. 1). The impact of forest use was taken into account by summarising historical records of land-use and canopy disturbances. Anthropogenic activities in the forest were compiled from diverse publications, unpublished documents, and forest reports dealing with forest administration and land-use history (see also Linares and Tíscar 2010). Next, we used this review to avoid, as much as possible, forests disturbed by anthropogenic influences, such as intensive loggings or fires, in order to focus on the climate–growth relationship.

The bedrock of the region is composed primarily of dolomite and limestone. The main soil types are leptosols (rendzinas) on higher slopes and luvisols on flat terrain with alluvial and colluvial deposits (Alejano and Martínez 1996). *P. nigra* co-occurred with *Quercus ilex* L. and *Q. faginea* Lam. in all study sites. At lower elevations, Mediterranean species (*Rosmarinus officinalis* L., *Juniperus oxycedrus* L. and *Pistacia terebinthus* L.) were common, whereas sub-Mediterranean species (*Daphne laureola* L., *Juniperus communis* L., *Berberis vulgaris* L. and *Crataegus monogyna* Jacq.) were more frequent from mid-elevation upwards.

Climatic data

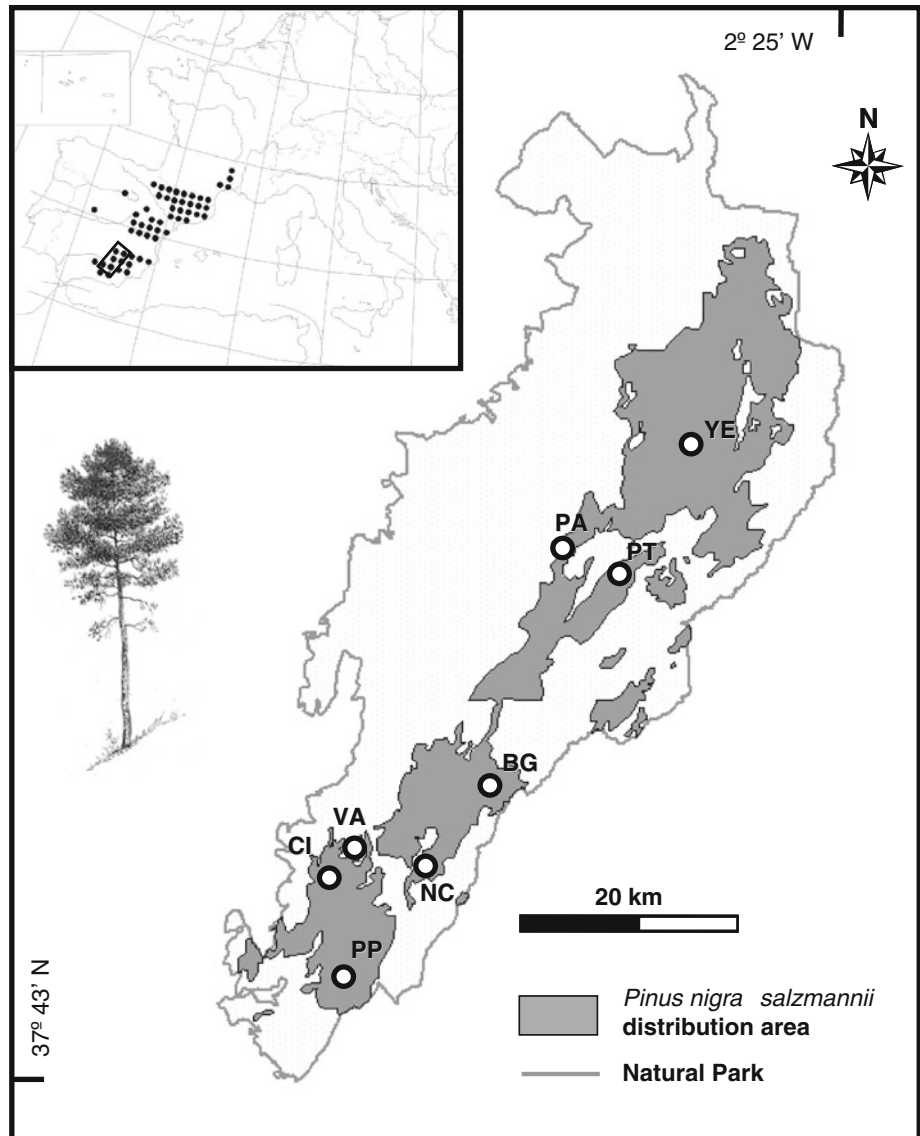
We used regional precipitation and temperature data for the period 1799–2004 reconstructed from original instrumental and documentary sources; tree-ring series were not used in any of these reconstructions. Regional precipitation data for the period 1799–1997 were obtained from indices of reconstructed regional precipitation from Rodrigo et al. (1999). Historical weather records were obtained by the analysis of original documents from a variety of sources: urban annals; city histories; general histories of Spain; religious chronicles; brief reports of events and letters; and books of church and city archives. Furthermore, the longest instrumental series in the Iberian Peninsula is the rainfall series for Gibraltar (ca. 300 km from our study area), covering the period 1791 to the present, which matched our modelled tree-ring span (1799–2004).

For this precipitation database, monthly regional indices were established by averaging the monthly values corresponding to each locality. A seasonal index was then formulated by averaging monthly values. The seasonal and annual indices were defined as: winter, December (of the previous year) + January + February; spring, March + April + May; summer, June + July + August; autumn, September + October + November; annual index, sum of the four seasonal indices. The index values were derived from instrumental sources based on the percentile distributions of rainfall in several instrumental series (P = rainfall; P_i = i th percentile of the instrumental series, assigned value appears in parentheses): Very dry (−2): $P < P_{i10}$; Dry (−1): $P_{i10} < P < P_{i25}$; Normal (0): $P_{i25} < P < P_{i75}$; Wet (+1): $P_{i75} < P < P_{i90}$; Very wet (+2): $P > P_{i90}$. The database is available at:

http://www.ucm.es/info/reclido/es/basesdatos/andalusian_rainfallindex.htm.

Since the used regional precipitation dataset reaches to 1997, this time series was completed for the period 1998–2004 by linear regression using the above-mentioned rainfall indices and rainfall data from the Gibraltar

Fig. 1 Distribution of *Pinus nigra* ssp. *salzmannii* forests in Europe (inset) and study sites (circles) along the Sierra de Cazorla, Segura y Las Villas Natural Park, SE Spain. The shading areas indicate the approximate *P. nigra* ssp. *salzmannii* range in the study area



meteorological station, provided by GHCN, National Climatic Data Center, USA) available at:

<http://www.ncdc.noaa.gov/ghcnm/>.

Regional temperature data for the period 1799–2004 were taken from Luterbacher et al. (2004) and Xoplaki et al. (2005). Here, European seasonal temperature was reconstructed on the basis of monthly instrumental temperature time series in combination with temperature index series derived from documentary evidence. This dataset is part of The NOAA Paleoclimatology Program. For more information about European Seasonal Temperature Reconstructions, see:

<ftp://ftp.ncdc.noaa.gov/pub/data/paleo/historical/europe-seasonal.txt>.

To estimate an integrative drought index (DI hereafter, see Eq. 1), we calculated the additive effect of temperature and precipitation as the difference of the normalised values

of annual mean temperature minus the annual rainfall index:

$$DI_i = T_{Ni} - P_{Ii} \tag{1}$$

where DI_i is the estimated drought index for the year i ; T_{Ni} is the normalised mean annual temperature of the year i , estimated as:

$$T_{Ni} = \frac{T_i - T_M}{T_{SD}} \tag{2}$$

where T_i is the mean annual temperature of the year i , T_M is the mean temperature for the period 1799–2004, and T_{SD} is the temperature standard deviation for the period 1799–2004, while P_{Ii} is the annual rainfall index of the year i , as we defined above. The same compute procedure was used to estimate seasonal drought indexes.

T_N reaches values of about -2 for cool years and values of about $+2$ for hot years. On the other hand, the annual rainfall index reaches values of -8 in very dry years (if the four seasons of this year showed very dry conditions) and values of $+8$ in very wet years (if the four seasons of this year showed very rainy conditions; see annual rainfall index definition above). It should be noted that, since we have not normalised the rainfall index, the P_I scores have about threefold the variation of T_N , and thus P contributes more than T to our drought index. In summary, DI yields minimum drought values (to -10 for higher water availability) if a given cool year matched with wet conditions, and maximum drought values (to $+10$ for extreme drought events) if a given hot years matched with dry conditions (see Eq. 1).

The temporal trends of the seasonal mean temperature and seasonal total precipitation were estimated using the Mann–Kendall test (Mann 1945; Kendall 1975). Mann–Kendall tests are non-parametric tests for the detection of a trend in a time series. The null hypothesis of this analysis assumes that the trend of the time series is zero and is rejected if the

absolute value of the Mann–Kendall statistic is higher than 1.96 for a two-tailed test at 95% significance or 2.58 at 99% significance. The sign of the Mann–Kendall statistic indicates whether the trend is positive or negative. The Mann–Kendall test also yields a summarised trend of the data via estimation of the multivariate analyses of the seasonal data, which were interpreted in this paper as a summarised annual trend (see Libiseller and Grimvall 2002). The analyses were performed using a free application download from:

<http://www.ida.liu.se/divisions/stat/research/Software/index.en.shtml>.

Sub-regional temperature and precipitation were documented from several meteorological stations over the study area (see Linares and Tíscar 2010). Based on documentary sources and an extensive field survey, we selected four habitat types representative of the average *P. nigra* climate range. Each site type was replicated with two populations at least 10 km apart (see Fig. 1; Table 1). Habitat types were operationally defined as: Cool/Wet type: high-elevation sites with mean temperature around 9°C and a mean

Table 1 Mean characteristics of the *Pinus nigra* ssp. *salzmannii* populations studied along the Sierra de Cazorla, Segura y Las Villas Natural Park, SE Spain

Plot (site type)	PP (Cool/Wet)	BG (Cool/Wet)	CI (Warm/Wet)	NC (Warm/Wet)	PT (Cool/Dry)	YE (Cool/Dry)	VA (Warm/Dry)	PA (Warm/Dry)
Latitude (N)	37°49'	37°55'	37°53'	37°54'	38°03'	38°15'	37°55'	38°06'
Longitude (W)	2°58'	2°48'	2°58'	2°52'	2°44'	2°39'	2°57'	2°52'
Elevation (m a.s.l.)	1,819 ± 21	1,699 ± 25	1,211 ± 71	1,435 ± 18	1,633 ± 20	1,600 ± 21	1,133 ± 36	1,016 ± 11
Slope (%)	24 ± 4	26 ± 3	30 ± 5	25 ± 5	23 ± 5	21 ± 1	20 ± 7	29 ± 7
Aspect	E–NE	W–NW	E–NE	N–NE	S–SW	E–SE	N–NE	N–NW
Mean temperature (°C)	8.95	9.38	11.52	10.45	9.63	9.76	11.95	12.64
Total annual precipitation (mm)	1,393	1,278	1,172	1,219	1,149	975	1,123	939
DBH (cm)	61 ± 8	80 ± 5	62 ± 2	64 ± 12	74 ± 8	61 ± 7	74 ± 1	72 ± 2
Age DBH (years)	242 ± 43	204 ± 23	145 ± 5	222 ± 48	156 ± 22	207 ± 36	138 ± 8	126 ± 6
Mean within tree BAI variance	27.81 ± 7.38	118.72 ± 23.58	51.11 ± 6.53	66.46 ± 13.50	101.36 ± 21.32	87.07 ± 25.69	38.52 ± 7.31	30.77 ± 7.22
Mean within stand (among trees) BAI correlation	0.60 ± 0.04	0.66 ± 0.02	0.42 ± 0.05	0.46 ± 0.06	0.51 ± 0.05	0.51 ± 0.06	0.45 ± 0.03	0.52 ± 0.06

Values are means ± SE. Four site types representative of the average *P. nigra* climate range were defined, noted in the first row in parentheses. Mean within-tree BAI variance was calculated as the variance of the annual BAI values (i.e. variance of the BAI for a given tree) for the period 1950–2000; individual variance values were then averaged for each stand. Mean within-stand BAI correlation was calculated as the among trees BAI correlation (i.e. covariance of the BAI series among the trees sampled for a given stand) for the period 1950–2000; peer correlation values were then averaged for each stand

DBH Diameter at breast height (1.3 m from the base)

annual precipitation of about 1,300–1,400 mm; Warm/Wet type: low-elevation sites with a mean temperature around 11°C and a mean annual precipitation of about 1,200 mm; Cool/Dry type: high-elevation sites with a mean temperature of around 9.5°C and a mean annual precipitation of about 1,000–1,100 mm; and Warm/Dry type: low-elevation sites with mean temperature around 12°C and a mean annual precipitation of about 900–1,100 mm (Table 1). All eight sampled sites occupied intermediate positions on steep hillsides running down from rocky outcrops to mountain streams. This was done to avoid possible effects of topography on soil conditions, i.e. depth, allowing sub-regional temperature and precipitation, along with aspect and slope, to be the dominating factors in determining water availability at each site.

Field sampling and dendrochronological methods

At each selected stand (Fig. 1; Table 1), we roughly marked a plot (ca. 2–4 ha, depending on the geomorphology and stand structure) and selected the 10 apparently largest diameter and most dominant trees. We sampled dominant trees, avoiding those with asymmetrical growth and non-circular bole. Each tree was measured for stem circumference to determine the diameter at breast height (1.3 m from the base) and cored using a 40-cm increment borer. Just after collection, each sample was visually examined in the field for scars, wood rot and other anomalies, in which case the sample was discarded and the tree was re-sampled or excluded (see Woodall 2008).

Cores were sanded and visually cross-dated, and their ring-width series were measured to the nearest 0.001 mm with a stereomicroscope mounted above a Velmex “TA” System device linked to a computer. Cross-dating quality was checked using COFECHA (Holmes 1983). The trend due to the geometrical constraint of adding a volume of wood to a stem of increasing radius was corrected by converting tree-ring widths into basal-area increments (BAI). When a wood core did not reach the pith, we calculated basal area increment values as follows. First, we calculated the tree stem radius (Rad) from its perimeter value (Per) measured in the field at 1.3 m from the base, as $\text{Rad} = \text{Per}/2\pi$; Then, we obtained the radius inside bark (RadIB) as the difference between Rad and the bark thickness measured in the field. The difference between RadIB and the core length (CL) gives the radius of the stem just prior to the formation of the first tree-ring captured by the core. Thus, the stem basal area at that time (BA_0) can be estimated as:

$$\text{BA}_0 = \pi * (\text{RadIB} - \text{CL})^2 \quad (3)$$

The stem basal area by the end of the following year (the year of formation of the oldest tree-ring in the core) can be calculated as:

$$\text{BA}_1 = \pi * (\text{RadIB} - \text{CL} + \text{TRW}_1)^2 \quad (4)$$

where TRW_1 is the measured width of the oldest ring in the core. Therefore, the first basal area increment value in our time series is:

$\text{BAI}_1 = \text{BA}_1 - \text{BA}_0 = \pi * (\text{RadIB} - \text{CL} + \text{TRW}_1)^2 - \pi * (\text{RadIB} - \text{CL})^2$; the second one is:

$\text{BAI}_2 = \text{BA}_2 - \text{BA}_1 = \pi * (\text{RadIB} - \text{CL} + \text{TRW}_1 + \text{TRW}_2)^2 - \pi * (\text{RadIB} - \text{CL} + \text{TRW}_1)^2$, and so on.

Average stand BAI was calculated as the mean of the ten cored trees (Biondi and Qaedan 2008). BAI trends were calculated for different time periods by least squares linear regression. The differences among BAI trends were tested by two slopes comparison test (see Zar 1999), which compare the slopes and intercepts of two regression lines.

Data analyses and modelling

Dynamic factor analysis (DFA) was used to estimate common underlying patterns in the tree growth data. DFA analyses were applied to normalised BAI time series because this facilitates the interpretation of factor loadings and the comparison of regression parameters; BAI was normalised for each stand by subtracting the mean stand BAI and dividing by the standard deviation (see also Biondi and Qaedan 2008; Linares et al. 2010). This method provides for each population factor loadings, which indicate the weight of a particular trend in this time series. In addition, the comparison of factor loadings of different time series allows the detection of common BAI trends among different populations, which cannot be achieved by other ordination methods as principal component analysis. In DFA, the time series are modelled as a linear combination of stochastic non-linear trends (Harvey 1989), which describes trends better than models not conceived specifically for time series analysis (see Zuur et al. 2003).

The goodness-of-fit of the model was assessed by Akaike’s information criterion (AIC; Akaike 1974), which combines the measure of fit with a penalty term based on the number of parameters used in the model. DFA was implemented using the Brodgar ver. 2.4.1 statistical package (Highland Statistics, Newburgh, UK), which was linked to R software (R Development Core Team 2011). Further details about DFA may be found as Supplementary material and in Zuur et al. (2003).

We revised and summarised climate–growth correlation analysis and response functions published in previous studies that focused on *P. nigra* in Spain (Creus and Puigdefabregas 1983; Richter et al. 1991; Fernández et al. 1996; Martín-Benito et al. 2008; and references therein) to propose five climate–growth models as follows. First, we hypothesised that BAI trends could be explained by the combined effect of temperature and precipitation, as

expressed by the Drought Index (DI; see Eq. 1). We then used the DI of five consecutive seasons as explanatory variables: prior autumn (the autumn season immediately preceding the growing season), winter (the winter season immediately preceding the growing season), spring, summer and autumn. Then, we selected the most significant, but uncorrelated, among them (if two seasons were highly significant but correlated, only the season that explained more variance was included in the model).

Second, we hypothesised that BAI trends could be explained by the single effect of temperature. To test this, we used the normalised temperature from five consecutive seasons as an explanatory variable, using the same criteria given above for the first model.

Third, based on response functions established in the same study area by Martín-Benito et al. (2008, and references therein), we hypothesised that BAI trends could be explained by the combined effect of winter precipitation (positive effect), spring drought (based on reported negative effect of temperature and positive effect of precipitation for the months of spring), and autumn temperature (negative effect).

Fourth, based on response functions established for *P. nigra* by Richter et al. (1991), we hypothesised that BAI trends could be explained by the combined effect of prior autumn drought (based on the reported negative effect of temperature and positive effect of precipitation for the months of the prior autumn), winter temperature (positive effect), and spring drought (based on the reported negative effect of temperature and positive effect of precipitation for the spring).

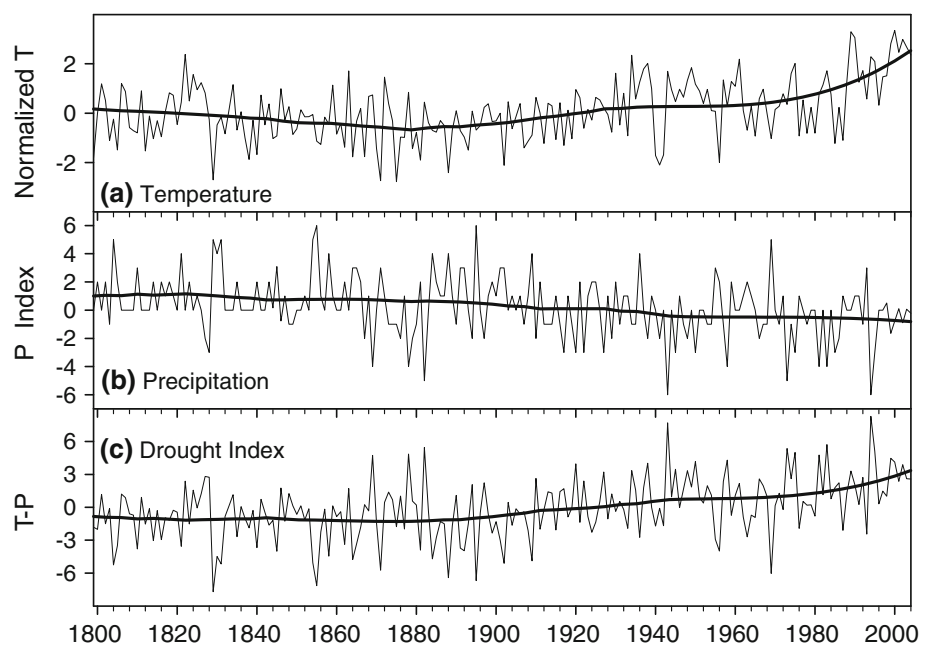
Fifth, a null model (constant BAI) was also tested (see Biondi and Qaedan 2008).

We fitted linear mixed-effects models using the nlme package in R software (R Development Core Team 2011). Climate variables explained above were included as fixed effects, and each tree was included as a random effect. The covariance parameters were estimated using the restricted maximum likelihood method, which makes estimates of parameters by minimising the likelihood of residuals from the fitting of the fixed effects portion of the model (see further details in Zuur et al. 2009). We used an information-theoretic approach (as has been described for DFA above) for multi-model selection, based on the AIC corrected for small sample sizes (AICc). We considered models with substantial support to be those in which the ΔAIC (i.e. the difference of AICc between models) was < 2 (see Burnham and Anderson 2002).

Results

Regional temperatures, precipitation, and the drought index are presented in Fig. 2. The Mann–Kendall test applied over the 1799–2004 span showed a significant increase in mean annual temperature mainly due to twentieth century warming (Mann–Kendall test = 5.57; $P < 0.001$; see Supplementary material, Fig. A1). Spring (March, April, and May) and winter (December, January and February) registered the greatest temperature increase, while summer (June, July and August) had the least significant increase, although this has strongly increased since 1970 (see Supplementary material, Fig. A1). Annual precipitation showed significant negative trends over the 1799–2004 span (see Supplementary material, Fig. A2). The greatest

Fig. 2 **a** Regional mean temperature normalized as the mean annual temperature minus the mean temperature for the period 1799–2004, divided by the temperature standard deviation for the period 1799–2004 (Xoplaki et al. 2005, Luterbacher et al. 2004). **b** Annual rainfall index (Rodrigo et al. 1999). **c** Drought index: temperature (a) minus precipitation (b). The thicker line represents long-term trends estimated by a local smoothing technique using polynomial regression and weights computed from the Gaussian density function (LOESS; see Zuur et al. 2009)



precipitation decrease was found in spring (Mann–Kendall test = -2.43 ; $P = 0.02$), while the summer precipitation trend was not significant.

All the trees studied were of similar size (~ 70 cm diameter); however, tree age at coring height and radial growth variance differed significantly (Table 1). The time span of the chronologies varied from ~ 100 to 400 years (data not shown); the older stands were located above 1,500 m. Correlation among trees within each stand, estimated for the period 1950–2000, was about 0.52 (ranging from 0.66 to 0.42), while average within-tree BAI variance, estimated for the same time period, yielded a very heterogeneous pattern (Table 1). The higher BAI correlation among trees was obtained in the two stands selected as Cool/Wet type (PP and BG, 0.63 on average) but these stands also showed the higher difference in mean within tree BAI variance (27 vs. 118 for PP and BG, respectively; Table 1).

Common BAI trends estimated by dynamic factor analysis are shown in Fig. 3. The model containing two common trends and a non-diagonal error covariance matrix

was the most suitable as judged by the AIC (data not shown). Trend 1 showed a steeply rising BAI, with a moderate increase between 1800 and about 1880, a sudden BAI rise from 1880 to 1890, and a moderate increase-to-steady BAI values thereafter. Trend 2 was characterised by a sustained BAI decline since the onset of the twentieth century (Fig. 3). Variation in BAI was significantly explained by one or both dynamic factor analysis trends (Table 2). Stands from sites with higher precipitation showed long-term BAI more related to trend 1 (increasing BAI), while stands from sites with lower precipitation showed higher loading factors for trend 2 (decreasing BAI; Table 2; Fig. 3); this indicates that drier stands followed a similar underlying declining growth pattern.

However, dynamic factor analyses also showed deviations from the common pattern stated above. Differences between peer of populations within some site types were noticeable, for instance in the Cool/Dry type, where YE population yielded higher affinity to Trend 1, which differs from the other three dry populations (PT, VA and PA). In the Cool/Wet type both PP and BG show little coupling to the trends, since the overall amounts of variance explained (Table 2) and the loading factors (Fig. 3) are small, although they show more variance explained by Trend 1 (increasing BAI), than by Trend 2. The NC site was coupled to both trends, but the loading factor for the Trend 2 (decreasing BAI) was negative (see Fig. 3), which indicates a clear positive growth trend for this Warm/Wet stand.

The mean values of environmental characteristics and BAI for the representative site types are shown in Table 3. Between 1800 and 1850, all the populations studied exhibited a similar and positive BAI trend. Between 1850 and 1900, the BAI trends remained similar and positive with the exception of the higher-elevation stands from the wet sites, which declined in growth over the second half of the nineteenth century. Since the beginning of the twentieth century, stands from drier sites showed declining growth trends that were significantly more pronounced for warmer stands; however, mean growth differences among the four stand types narrowed to non-significant differences in the second half of the Twentieth century (Table 3).

Linear mixed-effect modelling relating raw BAI data and climate was performed with respect to the four representative site types (see Table 4). For Cool/Wet type, the selected model explaining BAI was based on the prior autumn temperature, winter temperature, and autumn temperature. For Warm/Wet type, the selected model was also based on prior autumn temperature, but here spring temperature was the most significant predictor. For dry site types (both Cool and Warm), the selected model explaining BAI was based on prior autumn drought, spring drought, and autumn drought (Fig. 4; Table 5).

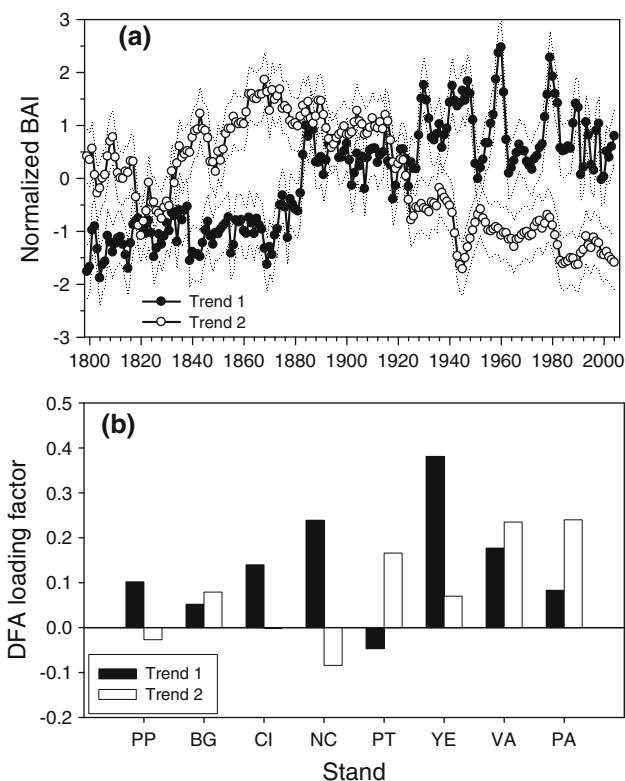


Fig. 3 Estimated trends (a) were established by dynamic factor analysis (DFA) for the normalised basal-area increment (BAI) of the eight studied *Pinus nigra* ssp. *salzmannii* populations. Dotted lines represent the 95% confidence interval. Loading factors (b) were determined by dynamic factor analysis and are shown for trend 1 (increasing BAI; black) and trend 2 (decreasing BAI; white)

Table 2 Basal area increment (BAI) variance explained by the two modelled common growth trends determined from dynamic factor analysis (DFA), in eight *Pinus nigra* ssp. *salzmannii* populations studied along the Sierra de Cazorla, Segura y Las Villas Natural Park, SE Spain

Plot (site type)	DFA common trend 1 (increasing BAI)		DFA common trend 2 (decreasing BAI)	
	Variance explained (%)		Variance explained (%)	
PP (Cool/Wet)	9.18	***	2.33	*
BG (Cool/Wet)	7.69	***	0.4	
CI (Warm/Wet)	14.21	***	2.58	*
NC (Warm/Wet)	68.29	***	44.99	***(-)
PT (Cool/Dry)	21.66	***	59.59	***
YE (Cool/Dry)	82.39	***	4.76	***
VA (Warm/Dry)	0.25		54.68	***
PA (Warm/Dry)	6.29	***	81.42	***

The stand type, based on local climate, appears in parentheses; (-) indicates that the long-term BAI pattern for this plot is negatively correlated to the modelled common trend

* $P < 0.05$, *** $P < 0.001$

Table 3 Mean characteristics and measured basal area increment (BAI) trends in the four stand types defined in the study

Site type	Cool/Wet	Warm/Wet	Cool/Dry	Warm/Dry
Mean temperature (°C)	9.16 ± 0.31	10.99 ± 0.76	9.69 ± 0.09	12.29 ± 0.49
Total annual precipitation (mm)	1,335 ± 81	1,195 ± 33	1,062 ± 123	1,030 ± 130
DBH (cm)	70.49 ± 13.8	63.05 ± 1.77	67.43 ± 8.64	73.04 ± 0.98
Age DBH (years)	222 ± 26	183 ± 54	181 ± 36	131 ± 8
Mean among trees BAI correlation	0.58	0.39	0.45	0.41
Mean BAI 1800–1850 (cm ²)	16.28 ± 0.28 b	9.47 ± 0.38 a	14.23 ± 0.32 b	19.31 ± 1.02 b
BAI Trend 1800–1850 (cm ² 10 year ⁻¹)	0.86 ab	1.06 ab	0.54 a	1.86 b
Mean BAI 1850–1900 (cm ²)	18.57 ± 0.40 b	13.74 ± 0.36 a	20.72 ± 0.35 b	33.16 ± 0.59 c
BAI Trend 1850–1900 (cm ² 10 year ⁻¹)	-0.83 a	1.23 b	1.15 b	0.97 b
Mean BAI 1900–1950 (cm ²)	17.72 ± 0.49 a	19.05 ± 0.52 ab	21.96 ± 0.48 b	26.67 ± 0.89 c
BAI Trend 1900–1950 (cm ² 10 year ⁻¹)	-0.29 c	1.46 d	-1.19 b	-3.16 a
Mean BAI 1950–2000 (cm ²)	17.63 ± 0.62 a	17.85 ± 0.42 a	17.99 ± 0.59 a	16.94 ± 0.35 a
BAI Trend 1950–2000 (cm ² 10 year ⁻¹)	1.09 c	0.52 c	-0.11 b	-0.48 a

Values are means ± SE. Different letters indicate significant differences among stand types within 50-year periods, determined by ANOVA ($P < 0.05$); differences among BAI trends were tested by two slopes comparison test ($P < 0.05$)

DBH Diameter at breast height (1.3 m from the base); Age DBH indicates the tree age at coring height

Discussion

Sub-regional variability in *P. nigra* climate–growth relationships

We hypothesised that long-term *P. nigra* growth responses to regional climate change could differ at a sub-regional scale. The BAI showed different patterns among populations related to temperature and precipitation across the sites sampled (Table 5). Our results agree with those of other studies suggesting that species responses to climate are not uniform over space (Miyamoto et al. 2010; Galiano et al. 2010; Sarris et al. 2010), and also indicate how these responses can vary over a gradient of local climatic

conditions (Table 3). These findings support the idea that large-scale endeavours based on models that assume uniform species responses to climate change over space may be overly simplistic (O'Neill et al. 2008).

Based on dynamic factor analyses, we have stated that wet and dry stands follow contrasting underlying growth trends, characterised by steady-to-rising BAI in the wetter stands and declining BAI in the drier ones (Table 2; Fig. 3). However, some differences found among populations within the same type were noticeable. The stand YE belonged to the Cool/Dry type; however, it yielded higher affinity to Trend 1 (increasing BAI), which differs from the other three dry populations (Fig. 3). While we made much effort to avoid forests disturbed by strong anthropogenic

Table 4 Model selection criteria for *Pinus nigra* ssp. *salzmannii* growth expressed as basal-area increment in the four studied stand types

Plot	Model	Variables	<i>k</i>	AICc	Δ <i>i</i>	L(<i>gi</i> / <i>x</i>)	Wi
Cool/Wet 20 trees (<i>n</i> = 5,840)	Warming increase	TpA + TW + TA	5	41,639	0.00	1.00	100
	Drought increase	DpA + DS + DSU	5	41,660	20.68	0.00	0
	Richter et al. (1991)	DpA + TW + DS	5	41,667	27.81	0.00	0
	Martín-Benito et al. (2008)	TA + PW + DS	5	41,706	67.09	0.00	0
	Null model	Ctant	2	41,740	100.52	0.00	0
Sum						1.00	
Warm/Wet 20 trees (<i>n</i> = 5,209)	Warming increase	TpA + TS	4	36,956	0.00	1.00	100
	Richter et al. (1991)	DpA + TW + DS	5	36,981	24.62	0.00	0
	Drought increase	DpA + DW + DS	5	36,983	26.34	0.00	0
	Martín-Benito et al. (2008)	TA + PW + DS	5	36,991	34.34	0.00	0
	Null model	Ctant	2	37,019	62.54	0.00	0
Sum						1.00	
Cool/Dry 20 trees (<i>n</i> = 5,310)	Drought increase	DpA + DS + DA	5	40,305	0.00	1.00	100
	Warming increase	TpA + TSU + TA	5	40,332	26.50	0.00	0
	Richter et al. (1991)	DpA + TW + DS	5	40,343	37.72	0.00	0
	Martín-Benito et al. (2008)	TA + PW + DS	5	40,382	77.09	0.00	0
	Null model	Ctant	2	40,510	204.91	0.00	0
Sum						1.00	
Warm/Dry 20 trees (<i>n</i> = 4,608)	Drought increase	DpA + DS + DA	5	35,414	0.00	1.00	100
	Warming increase	TpA + TSU + TA	5	35,519	105.18	0.00	0
	Richter et al. (1991)	DpA + TW + DS	5	35,571	157.09	0.00	0
	Martín-Benito et al. (2008)	TA + PW + DS	5	35,645	231.67	0.00	0
	Null model	Ctant	2	36,173	759.35	0.00	0
Sum						1.00	

The climate–growth relationship published by Richter et al. (1991) and Martín-Benito et al. (2008), and models related to temperature and a drought index were tested. A null model (*BAI* constant, see Biondi and Qaedan 2008) was also tested. The *k* column represents the number of parameter included in the model: the number of explaining variables plus one constant plus the error. Models and variables in bold correspond to models with substantial support

Δ*i* Difference in AICc (Akaike information criterion corrected for small sample) with respect to the best mode; *L(gi/x)* likelihood of a model *gi* given the data *x*, *Wi* relative probability that the model *i* is the best model for the observed data; *T* normalised temperature, *P* rainfall index, *D* drought index estimated as T–P; seasons: *pA* prior autumn, *W* winter, *S* spring, *SU* summer, *A* autumn of the current year; *Ctant* *BAI* constant

influences in order to focus on climate–growth relationships, this pattern may be due to logging and pruning, which we know occurred between the years 1960 and 1980.

Indeed, the YE stand (as well as PT and BG) showed several sudden *BAI* releases and suppressions (see within-trees *BAI* variance at Table 1; and Supplementary materials, Fig. A3), which might also weaken the climate–growth responses. Nevertheless, the percentage of *BAI* variance explained by the climate–growth models was not lower for the types including these stands (Table 5). The stands included in the Cool/Wet type (PP and BG) showed little coupling to the trends modelled by dynamic factor analysis, since the overall amounts of variance explained by common trends were small (Table 2). This result should be partially explained because the Trend 1 fits a steeply rising *BAI* (Fig. 3), but the stands included in the Cool/Wet type yielded negative *BAI* trends from 1850 to 1950

(Table 3), which may be due to slightly lower mean annual temperatures occurring between these years (Fig. 2).

Our results support the contention that *P. nigra* is a drought-sensitive species susceptible to increased temperature and decreased precipitation, both recorded in the region and predicted by climate models (IPCC 2007). However, long-term growth responses to climatic change are linked to local mean precipitation and therefore the capacity to adapt to climate change will likely vary for this species across rainfall gradients (Fig. 4). Tree-growth responses to warmer temperatures were negative at drier sites and positive at wetter sites (Table 4; Fig. 4). Similar observations have recently been made for lodgepole pines (*Pinus contorta* var. *latifolia*) from Canada by Miyamoto et al. (2010). Both low- and high-elevation *P. nigra* populations from drier sites were negatively correlated with prior autumn, current autumn, and spring drought indices.

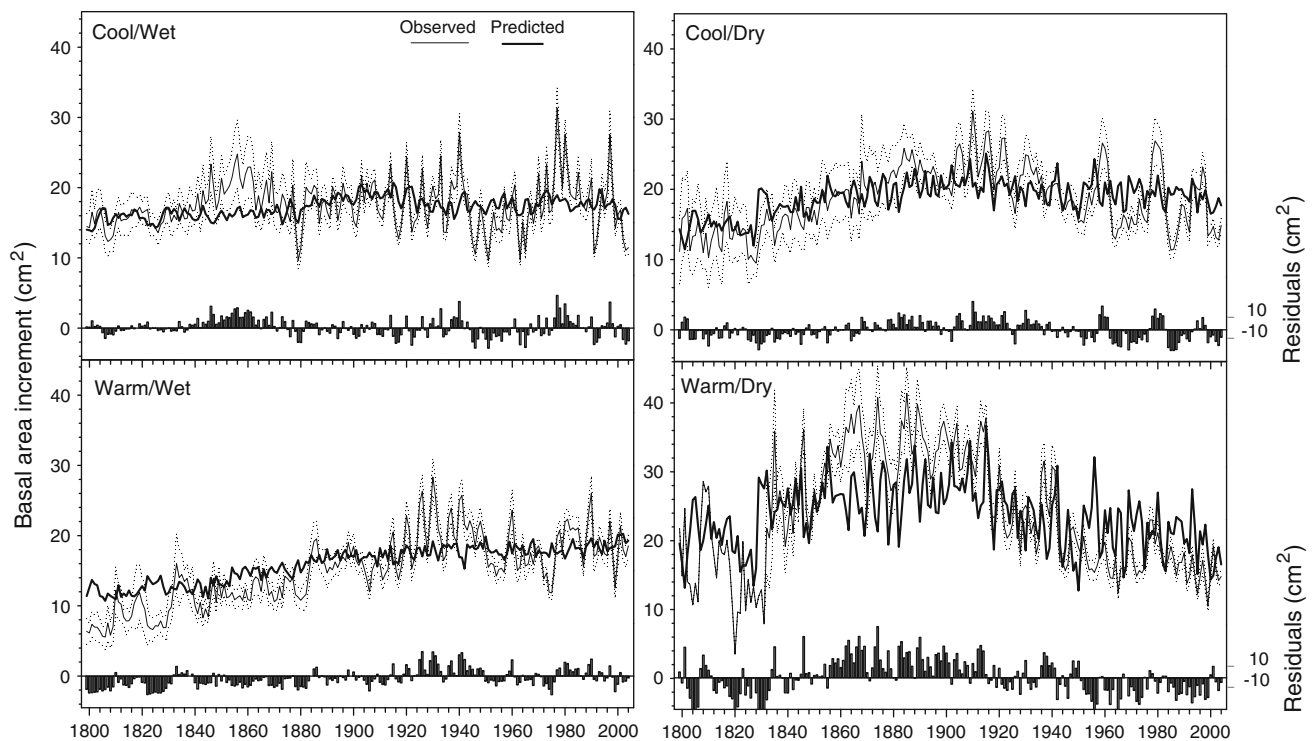


Fig. 4 Raw data of basal-area increment (*narrow line*) in the four stand types (two stands per type) and linear mixed-effect model (*thicker line*) fits based on climatic variables (see Table 4). *Bottom bar diagram* represents the residuals of the linear mixed-effect model,

expressed as the difference between observed minus predicted BAI values. The *inset* displays the stand type. *Dotted lines* represent the standard error

Table 5 Regression coefficients of the best-supported linear mixed-effects model explaining basal area increase (see also Table 4)

Independent variable	Type			
	Cool/Wet	Warm/Wet	Cool/Dry	Warm/Dry
TpA	-0.68 (54%)	0.52 (47%)		
TW	0.06 (5%)			
TA	-0.51 (41%)			
TS		0.60 (53%)		
DpA			-0.80 (42%)	-1.56 (31%)
DS			-0.67 (23%)	-1.45 (33%)
DA			-0.43 (35%)	-1.34 (31%)
Total variance explained (%)	41.18	33.07	35.40	27.43

TpA Prior autumn temperature, TW winter temperature, TA autumn temperature, TS spring temperature, DpA prior autumn drought index, DS spring drought index. For each variable, the relative weights in the model (%) appears in parentheses. Total variance explained is also noted

Previous dendrochronological studies also found *P. nigra* to be a drought-sensitive species (Richter et al. 1991; Martín-Benito et al. 2008; see also climate–growth functions taken from these authors in Table 4), although these models provided less support in our analysis. Results differing from those found in the analysis presented here could be explained perhaps as being based on standardised tree-ring-width series instead of BAI. In addition, we should consider that the sites and chronologies used by

these authors may differ to some extent from those used in our study.

Climate conditions in the autumn prior to active growth and in the spring were consistently and significantly correlated with *P. nigra* growth (Table 5). However, winter temperatures may also be important for assessing the potential impacts of climate change on stands at higher elevations. Model selection criteria (Table 4) suggest that *P. nigra* growth is broadly influenced by autumn (both

prior and current) as well as by spring drought in water-limited stands. Conversely, results suggest that warmer winters at cold sites and warmer springs at mild sites may enhance tree radial growth in stands with higher precipitation (Table 5). Warm winter temperatures may reduce cold temperature-induced foliage loss and root mortality, thereby maintaining better tree vigour favourable for early onset of growth and photosynthesis in warmer spring weather (Pederson et al. 2004). In addition, warmer winter and growing-season temperatures may enhance photosynthesis and carbohydrate allocation to the stem (McDowell et al. 2010). Although summer temperatures were not included in the models with higher support, the present data still suggest that warm summers are unfavourable for growth at both high- and low-elevation sites, since the growing season is arrested during these months (see Martín-Benito et al. 2008).

At lower elevations, temperature increases during the growing season were related to *P. nigra* growth decline in the twentieth century (Figs. 2, 4; Table 5; see also Supplementary materials). Rising temperatures increase the vapour-pressure deficit and evaporation, resulting in greater water loss through transpiration. Moreover, temperature rises may affect the *P. nigra* carbon storage in a particularly negative way because the rate of carbohydrate consumption required to maintain cell metabolism (respiration) is strongly linked to temperature (McDowell et al. 2010; Adams et al. 2009). This hypothesis could be supported by the less marked growth decline observed at higher elevations in water-limited sites (Table 3; Fig. 4), where lower mean temperatures might prevent or alleviate warming-related water stress.

Climate change and mediterranean mountain forests

Given drought sensitivity and temperature-induced stress of water-limited populations (Adams et al. 2009), the role of drought in shaping communities and affecting selection pressures in the Mediterranean mountain forest, as well as other drought-prone systems, will likely become even more important in a global-warming scenario (Parmesan 2006). Recently, several studies have linked tree-growth decline with increasing dryness in the Mediterranean Basin (e.g. Jump et al. 2006; Sarris et al. 2007, 2010; Piovesan et al. 2008; Linares et al. 2011; Galiano et al. 2010), suggesting a widespread climate change-related growth decline in several Mediterranean forests.

Annual precipitation showed a significant negative trend over the last two centuries (see Supplementary material, Fig. A2). In addition, the greatest precipitation decrease was found in spring, which was strongly related to *P. nigra* secondary growth (Table 5; Fig. 4). The drought index (Fig. 2c) indicates severe drought events,

characterised by high temperatures and low precipitation, around 1880, in the early 1940s and spanning the latter quarter of the twentieth century (about 1975–1995). Moreover, our analysis of the nineteenth to twentieth centuries on a regional scale showed the greatest temperature increases for spring and winter, while summer temperatures exhibited a pronounced increase since 1970 (see Supplementary material, Fig. A1). Based on the *P. nigra* climate–growth relationships found (Table 5; Fig. 4), consistently higher temperatures at the century-scale, matching with successive and severe droughts, may explain the declining growth trends and recent *P. nigra* die-off at drier sites (see Supplementary materials, Figs. A4, A5 and A6).

Long-term warming and increasing droughts can alter community structure and function (Aitken et al. 2008; Galiano et al. 2010). Moreover, land-cover changes greatly influence surface-energy balances and consequently climate (Bala et al. 2007). Indeed, the effects of land-cover changes have recently been associated with the persistent predictions of warming and drying throughout the Mediterranean Basin (Rotenberg and Yakir 2010). Variations in surface-radiation regimes and convective heat, derived from land-cover changes, can have considerable impacts on local, regional, and ultimately global climatic conditions (Bonan 2008). Drought-induced tree decay and mortality in the Mediterranean region might be associated with a considerable increase in albedo which, in turn, could result in reduced cloud convective activity that further promotes desertification (Rotenberg and Yakir 2010).

Concluding remarks

Forest vulnerability to climate change is still uncertain because different growth responses may differentially alter species dynamics and competitive interactions. Long-term changes in climate–growth relationships among coexisting drought-sensitive and drought-adapted tree species may eventually be expressed through shifts in forest composition and species distributions across multiple spatial and temporal scales. Wetter sites at both higher and lower elevations could show steady or even positive growth for *P. nigra* in response to rising temperatures, whereas for drier and warmer sites, impending *P. nigra* decline, regression, and progressive replacement by better drought-adapted Mediterranean taxa could be expected.

Acknowledgments The authors are grateful to Dr. J.J. Camarero for dendro-ecological advice and comments; we would also like to thank David Nesbitt for English revision. Consejería de Medio Ambiente (Junta de Andalucía) provided the means to carry out the field work. We also want to thank Dr. R. K. Monson and two anonymous reviewers for their comments which helped to improve a previous version of the manuscript.

References

- Adams HD, Guardiola-Claramonte M, Barron-Gafford GA, Villegas JC, Breshears DD, Zou CB, Troch PA, Huxman TE (2009) Temperature sensitivity of drought-induced tree mortality: implications for regional die-off under global-change-type drought. *Proc Natl Acad Sci USA* 106:7066–7067
- Aitken SN, Yearman S, Holliday JA, Wang T, Curtis-McLane S (2008) Adaptation, migration or extirpation: climate change outcomes for tree populations. *Evol Appl* 1:95–111
- Akaike H (1974) A new look at statistical model identification. *IEEE Trans Automat Contr* 19:716–722
- Alejano R, Martínez E (1996) Distribución de *Pinus nigra* Arn. ssp. *salzmannii* en las Sierras Béticas. *Ecología* 10:231–241
- Andreu L, Gutiérrez E, Macias M, Ribas M, Bosch O, Camarero JJ (2007) Climate increases regional tree-growth variability in Iberian pine forests. *Glob Change Biol* 13:1–12
- Bala G, Caldeira K, Wickett M, Phillips TJ, Lobell DB, Delire C, Mirin A (2007) Combined climate and carbon-cycle effects of large-scale deforestation. *Proc Natl Acad Sci USA* 104:6550–6555
- Biondi F, Qaadan F (2008) A theory-driven approach to tree-ring standardization: defining the biological trend from expected basal area increment. *Tree Ring Res* 64(2):81–96
- Bonan GB (2008) Forests and climate change: forcings, feedbacks, and the climate benefits of forests. *Science* 320:1444–1449
- Burnham KP, Anderson DR (2002) Model selection and multimodel inference: a practical information-theoretic approach. Springer, Heidelberg
- Creus J, Puigdefabregas J (1983) Climatología histórica y dendrocronología de *Pinus nigra*. In: Blanco A (ed) *Avances de Investigación en Bioclimatología*. CSIC, Zaragoza, pp 121–128
- Das AJ, Battles JJ, Stephenson NL, van Mantgem PJ (2007) The relationship between tree growth patterns and likelihood of mortality: a study of two tree species in the Sierra Nevada. *Can J For Res* 37:580–597
- Fernández A, Génova M, Creus J, Gutiérrez E (1996) Dendroclimatological investigation covering the last 300 years in central Spain. In: Dean JS, Meko DM, Swetman TW (eds) *Tree rings environment and humanity radiocarbon*. University of Arizona, Tucson, pp 181–190
- Galiano L, Martínez-Vilalta J, Lloret F (2010) Drought-induced multifactor decline of Scots pine in the Pyrenees and potential vegetation change by the expansion of co-occurring oak species. *Ecosystems* 13(7):978–991
- Harvey AC (1989) Forecasting structural time series models and the kalman filter. Cambridge University Press, Cambridge
- Holmes RL (1983) Computer-assisted quality control in tree-ring dating and measurement. *Tree Ring Bull* 43:68–78
- IPCC (2007) Climate change fourth assessment report. Cambridge University Press, London
- Jump AS, Hunt JM, Peñuelas J (2006) Rapid climate change-related growth decline at the southern range edge of *Fagus sylvatica*. *Glob Change Biol* 12:1–12
- Kendall MG (1975) Rank correlation methods. Charles Griffin, London
- Libiseller C, Grimvall A (2002) Performance of partial mann kendall tests for trend detection in the presence of covariates. *Environmetrics* 13:71–84
- Linares JC, Tiscar PA (2010) Climate change impacts and vulnerability of the southern populations of *Pinus nigra* subsp. *salzmannii*. *Tree Physiol* 30:795–806
- Linares JC, Camarero JJ, Carreira JA (2010) Competition modulates the adaptation capacity of forests to climatic stress: insights from recent growth decline and death in relict stands of the Mediterranean fir *Abies pinsapo*. *J Ecol* 98:592–603
- Linares JC, Camarero JJ, Delgado-Huertas A, Carreira JA (2011) Climatic trends and different drought adaptive capacity and vulnerability in a mixed *Abies pinsapo*–*Pinus halepensis* forest. *Clim Change* 105:67–90
- Luterbacher J, Dietrich D, Xoplaki E, Grosjean M, Wanner H (2004) European seasonal and annual temperature variability, trends and extremes since 1500. *Science* 303:1499–1503
- Macias M, Andreu L, Bosch O, Camarero JJ, Gutiérrez E (2006) Increasing aridity is enhancing silver fir *Abies alba* (Mill.) water stress in its south-western distribution limit. *Clim Change* 79:289–313
- Mann HB (1945) Nonparametric tests against trend. *Econometrica* 13:245–259
- Martín-Benito D, Cherubini P, del Río M, Cañellas I (2008) Growth response to climate and drought in *Pinus nigra* Arn. trees of different crown classes. *Trees Struct Funct* 22:363–373
- Martínez-Vilalta J, López BC, Adell N, Badiella L, Ninyerola M (2008) Twentieth century increase of Scots pine radial growth in NE Spain shows strong climate interactions. *Glob Change Biol* 14:2868–2881
- McDowell N, Allen CD, Marshall L (2010) Growth, carbon isotope discrimination, and climate-induced mortality across a *Pinus ponderosa* elevation transect. *Glob Change Biol* 16(1):399–415
- Miyamoto Y, Griesbauer HP, Green DS (2010) Growth responses of three coexisting conifer species to climate across wide geographic and climate ranges in Yukon and British Columbia. *For Ecol Manag* 259:514–523
- O'Neill GA, Hamann A, Wang T (2008) Accounting for population variation improves estimates of the impact of climate change on species' growth and distribution. *J Appl Ecol* 45:1040–1049
- Ogle K, Whitham TG, Cobb NS (2000) Tree-ring variation in pinyon predicts likelihood of death following severe drought. *Ecology* 81:3237–3243
- Parnesan C (2006) Ecological and evolutionary responses to recent climate change. *Annu Rev Ecol Evol Syst* 37:637–669
- Pederson N, Cook ER, Jacoby GC, Peteet DM, Griffin KL (2004) The influence of winter temperatures on the annual radial growth of six northern range margin tree species. *Dendrochronologia* 22:7–29
- Peñuelas J, Ogaya R, Boada M, Jump AS (2007) Migration, invasion and decline: changes in recruitment and forest structure in a warming-linked shift of European beech forest in Catalonia (NE Spain). *Ecography* 30:830–838
- Piovesan G, Biondi F, Di Filippo A, Alessandrini A, Maugeri M (2008) Drought-driven growth reduction in old beech (*Fagus sylvatica* L.) forests of the central Apennines, Italy. *Glob Change Biol* 14:1265–1281
- Richter K, Eckstein D, Holmes RL (1991) The dendrochronological signal of pine trees (*Pinus* spp.) in Spain. *Tree Ring Bull* 51:1–13
- Rodrigo FS, Esteban-Parra MJ, Pozo-Vázquez D, Castro-Diez Y (1999) A 500 year precipitation record in southern Spain. *Int J Climatol* 19:1233–1253
- Rotenberg E, Yakir D (2010) Contribution of semi-arid forests to the climate system. *Science* 327:451–454
- R Development Core Team (2011) R: A language and environment for statistical computing. R Foundation for Statistical Computing, Vienna, Austria. ISBN 3-900051-07-0, URL. <http://www.R-project.org>
- Sarris D, Christodoulakis D, Körner C (2007) Recent decline in precipitation and tree growth in the eastern Mediterranean. *Glob Change Biol* 13:1–14

- Sarris D, Christodoulakis D, Körner C (2010) Impact of recent climatic change on growth of low elevation eastern Mediterranean forest trees. *Clim Change* 106:203–223
- Taberlet P, Cheddadi R (2002) Quaternary refugia and persistence of biodiversity. *Science* 297:2009–2010
- van Mantgem PJ, Stephenson NL, Byrne JC, Daniels LD, Franklin JF, Fulé PZ, Harmon ME, Larson AJ, Smith JM, Taylor AH, Veblen TT (2009) Widespread increase of tree mortality rates in the western United States. *Science* 323:521–524
- Woodall CW (2008) When is one core per tree sufficient to characterize stand attributes? Results of a *Pinus ponderosa* case study. *Tree Ring Res* 64(1):55–60
- Xoplaki E, Luterbacher J, Paeth H, Dietrich D, Steiner N, Grosjean M, Wanner H (2005) European spring and autumn temperature variability and change of extremes over the last half millennium. *Geophys Res Lett* 32:L15713
- Zar JH (1999) *Biostatistical Analysis*. Prentice Hall, New Jersey
- Zuur AF, Fryer RJ, Jolliffe IT, Dekker R, Beukema JJ (2003) Estimating common trends in multivariate time series using dynamic factor analysis. *Environmetrics* 14:665–685
- Zuur AF, Ieno EN, Walker N, Saveliev AA, Smith GM (2009) *Mixed effects models and extensions in ecology with R*. Springer, New York